

Poly(o-anisidine) on brass: Synthesis and corrosion behavior

Ali Tuncay Ozyilmaz^{*,†}, Gul Ozyilmaz^{*}, Ercan Yılmaz^{**}, and Nureddin Çolak^{*}

^{*}The University of Mustafa Kemal, Arts and Science Faculty, Department of Chemistry, 31040 Hatay-Turkey

^{**}The University of Middle East Technical, Arts and Science Faculty, Department of Physic, 06531 Ankara-Turkey

(Received 30 March 2007 • accepted 19 December 2007)

Abstract—The electrochemical synthesis of poly(o-anisidine) (POA) was achieved on brass (CuZn) electrode by applying two scan rates (50 and 20 mVs⁻¹). The synthesized polymer films were strongly adherent and homogeneous in both cases. Their corrosion performance was investigated by AC impedance spectroscopy (EIS) technique, anodic polarization plots and open circuit potential-time curves, in 3.5% NaCl solution. It was clearly seen that poly(o-anisidine) films provided a significant physical protection for longer exposure time. It was shown that polymer film coated at high scan rate (CuZn/POA-H) exhibited better barrier property against the attack of corrosive agents when compared with polymer film obtained at low scan rate (CuZn/POA-L). It was found out that poly(o-anisidine) film synthesized at high scan rate caused a significant increase in corrosion resistance by its catalytic behavior on formation of protective oxide layers on the surface in longer time.

Key words: Coatings, Corrosion, Brass, Poly(o-anisidine), AC Impedance

INTRODUCTION

In industry, metals and their alloys have been widely used in numerous applications for many years. Their protection against corrosion has been investigated by several researchers [1-3]. Copper and copper alloys are protected means of quite a few methods such as organic inhibitor, organic coating and metallic plating [4-8].

Modification of oxidizable metal surfaces by electrochemical polymerization of organic compounds, such as pyrrole, aniline and their derivatives has been the subject of much attention in recent years. The resulting films are generally homogeneous, chemically stable and strongly adherent to the electrode surface. Conducting polymers have attracted much interest in the development of corrosion resistance and consequently can be used to protect metal against corrosion [9-11]. Polyaniline and its derivatives are mainly used as coating to improve the corrosion resistance of oxidizable metals. These coatings have also been considered for several applications such as the electronic industry, biosensor applications [12-17]. Borole et al. [18] studied the synthesis of the copolymerization of aniline and o-anisidine in various inorganic and organic supporting electrolytes in aqueous medium and focused on the investigation of the influence of various supporting electrolytes on the electrochemical synthesis of copolymers. Pawar et al. [19] investigated the electrochemical synthesis of poly(o-anisidine) on mild steel substrates under galvanostatic conditions from aqueous solutions of oxalic acid. Their work clearly revealed that the synthesized POA films were uniform and dark green.

The purpose of this study was to synthesize the adherent poly(o-anisidine) films on brass in 0.1 M o-anisidine containing sodium oxalate solution. Afterwards, the corrosion performance of brass electrode with and without poly(o-anisidine) was investigated in 3.5% NaCl.

EXPERIMENTAL

All the chemicals were purchased from Merck and o-anisidine was freshly distilled and stored in the dark. Solutions were prepared with distilled water and all experiments were carried out at room temperature open to the atmosphere. In this study, all the electrochemical experiments were performed in a single compartment cell with three electrode configurations. The reference electrode was an Ag/AgCl (sat, KCl) electrode and the counter electrode was a platinum sheet with a surface area of 2 cm². A CHI 660b model electrochemical analyzer (serial number: A1420) under computer control was used in electrochemical experiments. All of the potential values were referred to the Ag/AgCl (sat, KCl) electrode. The working electrode had a brass surface (CuZn) measuring 0.5 cm in diameter. The brass used in study was comprised of (w/w%): 57.76 Cu, 39.59 Zn, 0.28 Sn, 0.26 Fe, 0.12 Ni, 0.03 Al, 0.01 Mn, 0.02 Sb and 1.82 Pb.

Brass electrodes were embedded in a thick polyester block. In order to remove any existing passive film, the surface of working electrodes was polished by using up to 1200 grade emery paper before each experiment and electropolymerization, then rinsed in 1 : 1 ethanol acetone mixture, washed with bi-distilled water and dried.

The POA coating was synthesized with the help of cyclic voltammetry technique. Electrochemical impedance spectroscopy, open circuit potential (E_{ocp})-time curves and anodic polarization curves were used to investigate the corrosion performance of the coating. The Nyquist plots were recorded at instantaneous open circuit potentials for various exposure times and in the frequency range from 10⁵ to 10⁻³ Hz by using the amplitude of 7 mV. Scanning electron microscopy (SEM) was employed to characterize the surface morphology with JEOL JSM-5500LV Scanning electron microscope.

RESULTS AND DISCUSSION

1. Synthesis

[†]To whom correspondence should be addressed.

E-mail: atuncay@mku.edu.tr

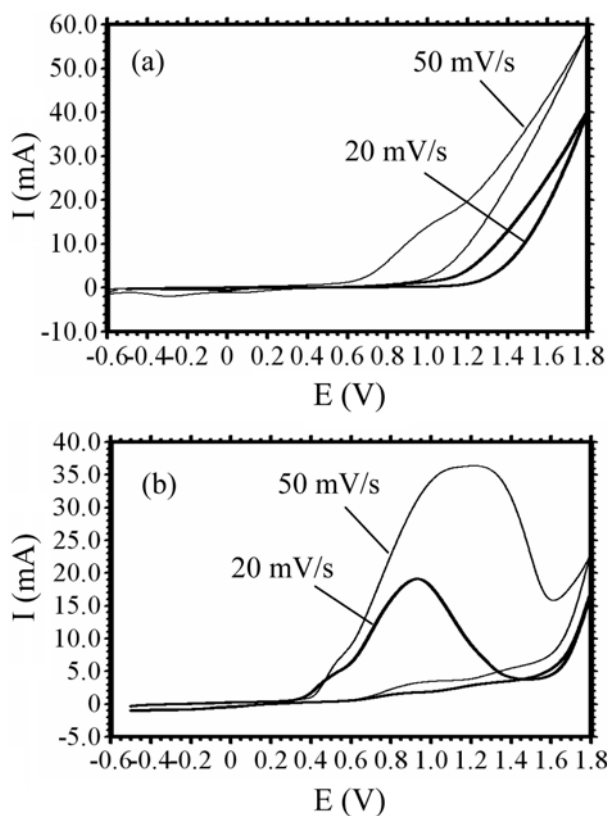


Fig. 1. The cyclic voltammograms recorded for Pt electrode in 0.2 M $\text{Na}_2\text{C}_2\text{O}_4$ (a) and 0.2 M $\text{Na}_2\text{C}_2\text{O}_4$ +0.1 M o-anisidine solution (b).

The cyclic voltammograms recorded for Pt electrode in sodium oxalate solution with and without monomer are given in Fig. 1(a) and 1(b), respectively. Measurements were taken at scan rates of 20 and 50 mV s^{-1} . In monomer-free solution, current values for 50 mV s^{-1} and 20 mV s^{-1} remained constant from approx. -0.60 V up to $+0.60$ V and 1.10 V, respectively. Anodic current increase recorded for both cases resulted from Pt oxides developed on Pt electrode. Then, current values started to increase rapidly at the potential value of 1.45 V. This was attributed to oxygen gas evolution. At the reverse scan, the reduction of previously produced oxides was observed for both scan rates as a small cathodic reduction peak at between approx. -0.30 and $+0.38$ V. In presence of monomer, the monomer oxidation peaks for Pt electrode were observed at approx. $+0.93$ V for low scan rate and at approx. $+1.21$ V for high scan rate and the charge amounts of low and high scan rates were found to be 0.26 and 0.35 C, respectively.

Fig. 2 shows the first voltammograms recorded for the brass electrode in sodium oxalate solution with and without monomer. As can be seen in the first cycle, the active dissolution of brass for low and high scan rates started at approx. -0.16 V. These processes continued as enormous current increase and were completed at approx. $+0.36$ V for low scan rate and 0.46 V for high scan rate. Charge amounts obtained for passivation mechanism at low and high scan rates were found as 5.00×10^{-2} and 8.22×10^{-2} C, respectively. This passivation process involved formation of insoluble copper and zinc oxalate (K_p values are 2.9×10^{-8} for $\text{Cu}_2\text{C}_2\text{O}_4$ and 1.5×10^{-9} for $\text{Zn}_2\text{C}_2\text{O}_4$)

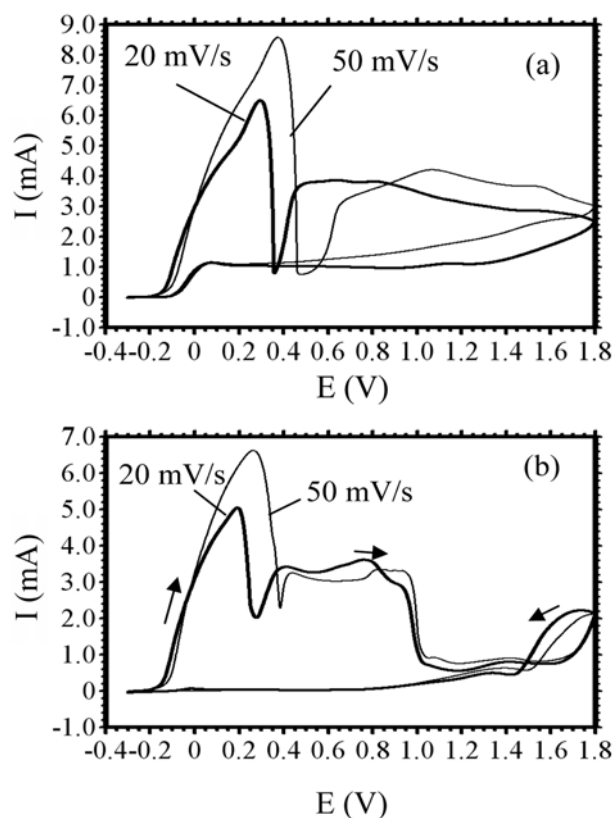


Fig. 2. The first cyclic voltammograms recorded for brass electrode at different scan rates in 0.2 M $\text{Na}_2\text{C}_2\text{O}_4$ (a) and 0.2 M $\text{Na}_2\text{C}_2\text{O}_4$ +0.1 M o-anisidine solution (b).

[20]. Thereafter, current values for both scan rates started to increase again partly due to further dissolution through the porous nature of the passive layer. The increase in current values was related to the formation of copper oxides (CuO and Cu_2O) on brass surface. In presence of monomer 0.1 M o-anisidine, the oxidation-passivation peak of brass electrode for both scan rates was observed between -0.21 and $+0.27$ V for low scan rate and between -0.20 and $+0.38$ V for high scan rate. Charge amounts recorded for low and high scan rates were found as 5.35×10^{-2} and 3.25×10^{-2} C, respectively. For both scan rates, these values recorded for the brass passivation in monomer medium were rather low when compared with those of monomer free mediums. This case was attributed to the inhibitor effect of o-anisidine on electrode surface. Then, current increments starting at approx. 0.27 V for low scan rate and at approx. 0.38 V for high scan rate were attributed to the oxidation of copper (I) oxides to copper (II) oxides on the brass surface. High current values obtained for the formation of Cu_2O and CuO made it clear that passivation of brass was not completed during oxidation/passivation process. Consequently, there were four passive layers such as copper and zinc oxalate complex compounds and copper (I, II) oxides on the brass surface before monomer oxidation process. The monomer oxidation process was observed at approx. 1.70 V. This peak for both scan rates was almost the same.

In Fig. 3, poly (o-anisidine) film growth was carried out in the potential range between $+0.30$ and 1.80 V and was achieved by applying 10 whole cycles for low scan rate and 25 whole cycles for

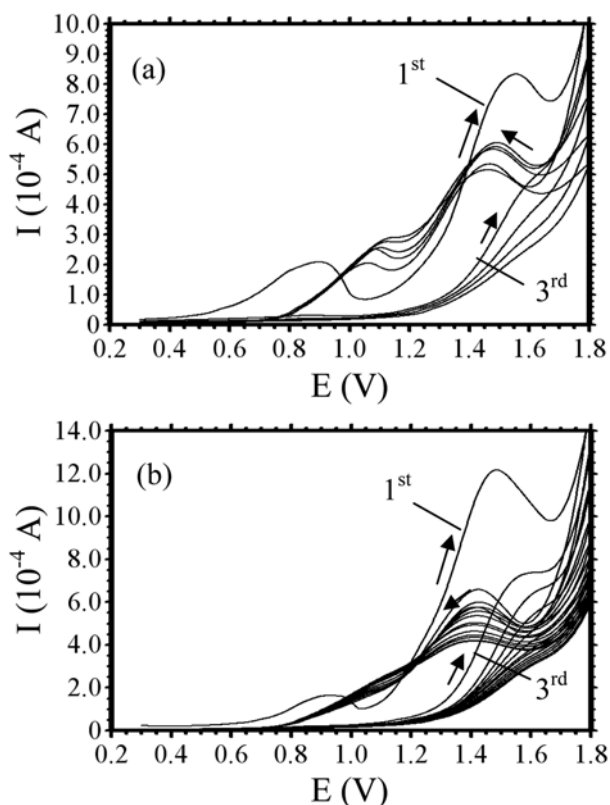
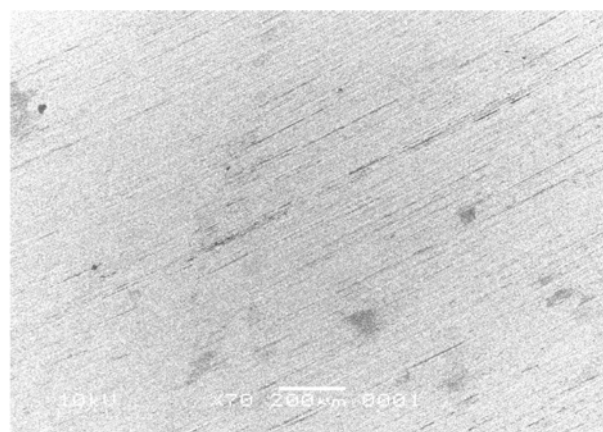


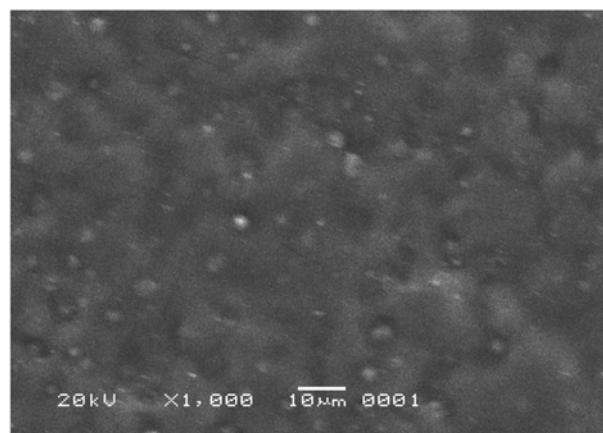
Fig. 3. The cyclic voltammograms recorded during the film growth on brass electrode in 0.2 M $\text{Na}_2\text{C}_2\text{O}_4$ +0.1 M *o*-anisidine, scan rates: 20 mVs^{-1} (a) and 50 mVs^{-1} (b).

high scan rate. Although the same duration was applied for synthesis of poly(*o*-anisidine) at different scan rates, the synthesized coatings had different thickness values such as 216 nm for low scan rate and 305 nm for high scan rate. The thickness of coatings was estimated from the sum of charges (Q) passing in monomer oxidation potential region in 10 whole cycles for low scan rate and 25 whole cycles for high scan rate [21]. It was clearly seen that the monomer oxidation peak was observed at the high potential region for each scan. Consequently, the upper potential limit was significant for polymer film growth in neutral medium [22,23]. It could be seen that the film growth curve recorded for poly(*o*-anisidine) coating produced in sodium oxalate solution exhibited similar behavior to that of poly(aniline-co-*o*-anisidine) film as well as polyaniline film [23-26]. The polymer film growth curves obtained for both scan rates were almost the same. Yet, their current values were relatively different and the current values recorded for low scan rate were relatively low when compared with those of high scan rate. Monomer oxidation peak intensities for both scan rates decreased regularly with continued scan and their peak potential values shifted to anodic region with increasing cyclic number. At the reverse scans, the transitions between the oxidation states of POA film were observed as well defined anodic two peaks in the potential ranges approx. 1.10 and 1.49 V. While the intensity of peaks recorded for synthesis of POA film showed a steady increase, initially, they decreased later on. Indeed, the electrode surface appeared to be covered with a dark black layer indicating the formation of POA.

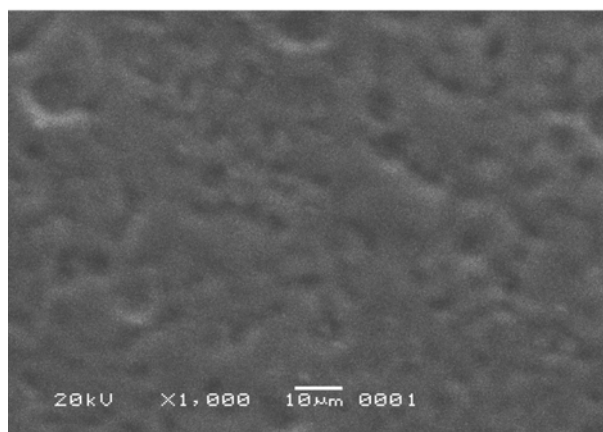
SEM images of bare brass and POA films synthesized on brass



(a)



(b)



(c)

Fig. 4. SEM images of uncoated (a), CuZn/POA-L (b) and CuZn/POA-H (c) brass electrodes.

electrode at both scan rates are shown in Fig. 4. It is clearly revealed that both POA coatings were relatively uniform and compact. On the other hand, poly(*o*-anisidine) film synthesized at high scan rate was strongly adherent and uniformly covered the entire electrode surface as evident by the SEM. In addition, the adherence of synthesized coatings was tested by a simple sello tape test and satisfactory results were obtained.

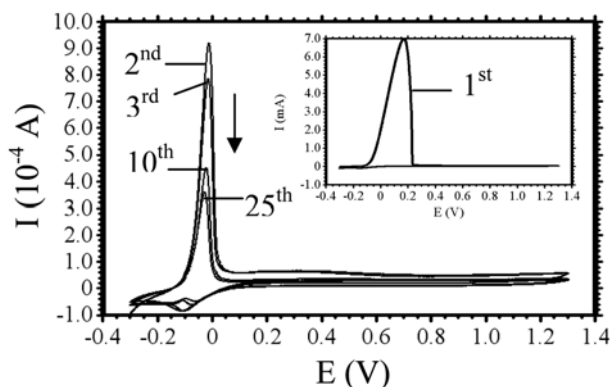


Fig. 5. Cyclic voltammograms of uncoated brass electrodes in monomer free 0.3 M oxalic acid solution. Inset: The first CV of the uncoated brass electrode.

2. Electrochemical Characterization of POA Films

Current-potential (CV) behavior of uncoated brass electrode is given in Fig. 5. In polymer free electrode during the first forward potential sweep, an oxidation peak between -0.14 and $+0.23$ V versus AgCl/Ag, resulting from electrodisolution of brass electrode was observed (see the insert on Fig. 5). Current value of this anodic peak at $+0.17$ V was found to be 7.0×10^{-3} A. Current values of uncoated electrode were observed to decline gradually for each scan with high peak intensity. Yet, it is clearly seen that the surface of brass electrode did not have complete passivation in oxalic acid medium. During reverse scan, the cathodic peak at -0.14 V was due to complex copper oxalate formation whereas oxalate anions reacted with remaining Cu (II) cation on the brass electrodes and its peak potential shifted to cathodic domain as current increment.

Fig. 6 shows the CVs of POA coated brass electrodes. POA coated brass electrodes were thoroughly rinsed and transferred to an o-anisidine free 0.3 M oxalic acid where cyclic voltammograms were traced in the potential region between -0.30 and 1.30 V at $dE/dt = 50$ mV s^{-1} . The curves of homopolymer coatings synthesized in two different scan rates on brass exhibited similar behavior. At the anodic scan of the first cycle, the oxidation/passivation peak was observed to be only one peak at approx. $+0.08$ V. Yet, there were two peaks which could not be well resolved from each other, during second and third anodic cycles. Afterwards, the feature of CVs consisted of well resolved two different peaks in the potential range -0.10 and $+0.20$ V during fifth scans of both POA coated electrodes. Anodic peak intensities corresponding to the oxidation/passivation at approx. $+0.06$ V decreased gradually during subsequent scans. The oxidation/passivation peak of both POA-coated electrodes was found to disappear after the thirteenth anodic cycle. As can be seen in Fig. 6(a) and 6(b) during subsequent scans, new anodic and cathodic peaks appeared which corresponded to the oxidation and reduction of POA films on the brass electrode surface. The intensities of these peaks increased during following cycles, indicating the build-up of an electroactive polymeric material (see the insert on Fig. 6(a) and 6(b)). The transitions between the oxidation states of polymer film were observed as the current increments in the potential range -0.05 V, while the current intensities of uncoated electrode decreased in the same potential region during subsequent scans. The anodic current approached an almost constant value of twenty-fifth anodic

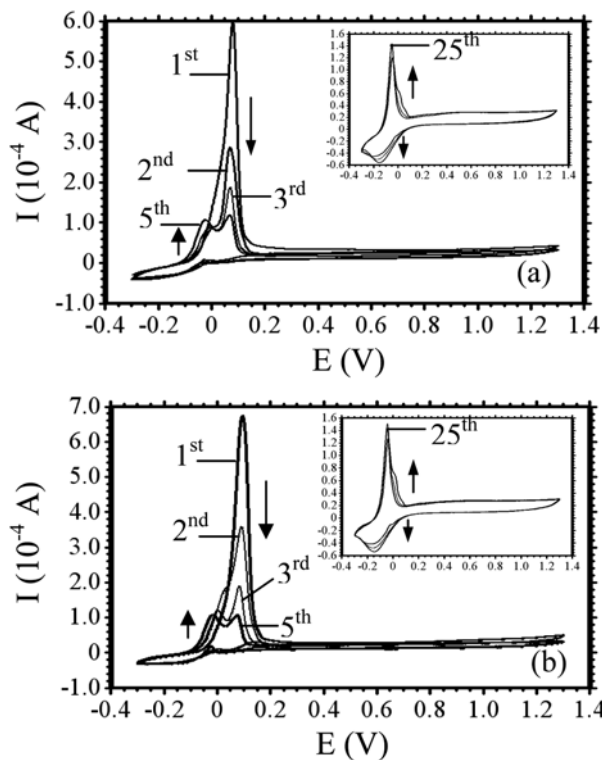


Fig. 6. Cyclic voltammograms of CuZn/POA-L (a) and CuZn/POA-H (b) coated electrodes in monomer free 0.3 M oxalic acid solution. Inset: The 10th, 15th and 25th CVs of the POA coated brass electrodes.

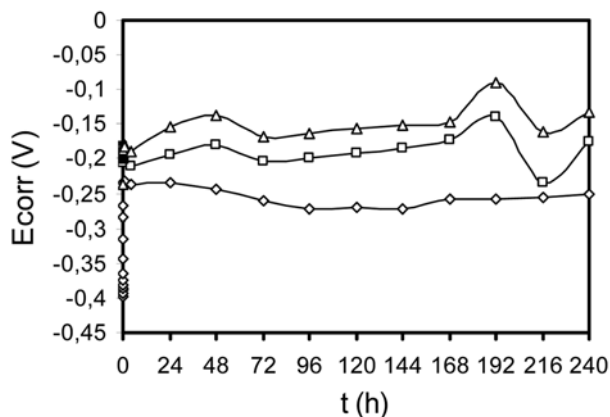


Fig. 7. The E_{corr} - t curves recorded for CuZn (\diamond) and CuZn/POA-L (\square) and CuZn/POA-H (\triangle) electrodes in 3.5% NaCl solution.

cycle.

3. Corrosion Behavior

The corrosion performance of bare brass (CuZn) and poly(o-anisidine) coated brass electrode (CuZn/POA) was investigated in 3.5% NaCl solution. The open circuit potential values (E_{ocp}) of uncoated and coated electrodes were monitored as a function of exposure time (Fig. 7). Brass electrodes coated at low and high scan rates will from now on be named as CuZn/POA-L and CuZn/POA-H, respectively. The initial E_{ocp} value of uncoated brass electrode

was -0.389 V. This value then started to increase with longer exposure time and remained constant at approx. -0.230 V after 4 h of immersion time. Initially, the surface dissolved and then passivated by insoluble CuCl and copper oxides. However, these passive layers could not resist against the attack of the chloride containing corrosive medium. After 240 h of immersion time, the E_{ocp} value of bare brass electrode was measured to be -0.252 V. The initial E_{ocp} values of polymer coated electrodes were rather nobler when compared with the bare brass electrode. The E_{ocp} values of CuZn/POA-L and CuZn/POA-H electrodes were measured to be -0.182 and -0.237 V, respectively. Then, the E_{ocp} values of CuZn/POA-H electrode started to increase rapidly by longer exposure time due to the buildup of stable copper oxide layers on the electrode, while E_{ocp} values of CuZn/POA-L electrode shifted to cathodic region. It was apparent that the polymer film synthesized at high scan rate on brass electrode exhibited an effective barrier property against corrosive agents such as dissolved oxygen and chloride ions. This could be simply explained with the formation of CuCl, CuO and Cu₂O on the brass surface [20,22]. This must be due to the catalytic effect of POA film on the passivation of brass [23,25-28]. It is already known that electroactive polymers behave as oxidizing inhibitor, when the limited electrolyte solution comes into contact with the underlying metal at the bottom of the pores. Consequently, while metal is oxidized as an anodic reaction, polymer film is reduced at the metal/polymer interface as well as hydrogen evolution and/or dissolved oxygen reduction as cathodic reaction. Furthermore, the catalytic behavior of electroactive polymer films is related to their porous structure. Therefore, because of less porous structure, the polymer film synthesized at high scan rate had more oxidizing effect when compared with the brass electrode coated at low scan rate. 240 h after the immersion time, The E_{ocp} values of CuZn/POA-L and CuZn/POA-H electrodes were measured to be -0.176 and -0.132 V, respectively. It was clearly observed that the E_{ocp} values of polymer coated electrodes moved to nobler region than that of uncoated brass electrode, in longer periods.

Fig. 8 shows the anodic polarization curves recorded for CuZn and CuZn/POA electrodes in 3.5% NaCl solution after 240 h of immersion time. In case of bare brass, the corrosion potential value (E_{corr}) was measured as -0.220 V. Current values increased up to

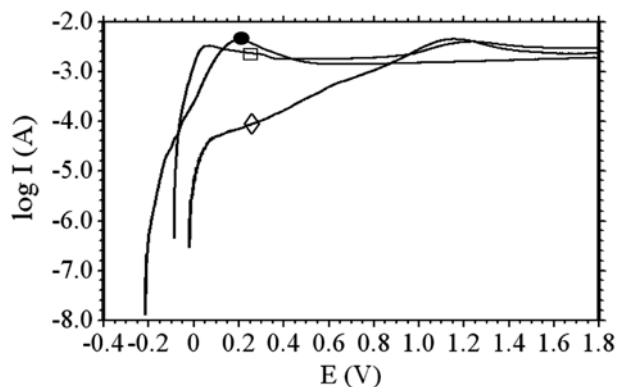


Fig. 8. The anodic polarization curves recorded for CuZn (●), CuZn/POA-L (□) and CuZn/POA-H (◇) electrodes, after 240 h of immersion time in 3.5% NaCl solution. Scan rate: 4 mV/s.

$+0.20$ V due to oxidation of the metal. It is apparent that the formation of stable CuCl and CuO/Cu₂O layers prompted a drop at the anodic current value due to the brass passivation. Then, the current value remained constant in potential domain between $+0.55$ V and $+0.91$ V. With continued potential, current values increased gradually after 0.91 V because of the activating effect of chloride ions on brass corrosion and led to partial breaking down of the passive layer. E_{corr} values of coated brass electrodes shifted to anodic region and these values were measured as -0.089 V for CuZn/POA-L and -0.019 V for CuZn/POA-H electrode. Positive E_{corr} values of polymer coated electrodes when compared with those of uncoated brass electrode rate were attributed to the barrier characteristic of the polymer coatings. Yet, CuZn/POA-H electrode exhibited a better physical barrier behavior than that of CuZn/POA-L electrode. It was clearly observed that the current values of CuZn/POA-H electrode in potential region between 0.07 V and 0.85 V were rather low than those of CuZn/POA-L electrode as well as bare brass electrode. Current increase beyond potential value of 0.93 V for both coated electrodes was evaluated as degradation of poly(o-anisidine) film.

Nyquist diagrams recorded for various immersion times in 3.5% NaCl solution for uncoated brass electrode are given in Fig. 9. As seen from Fig. 9, curves recorded for various immersion times were relatively different from each other. After 4 h of exposure time, there were two depressed semicircles which could not be well resolved from each other at high and medium frequencies in addition to an inductive loop at the low frequency region, in the Nyquist plot. The

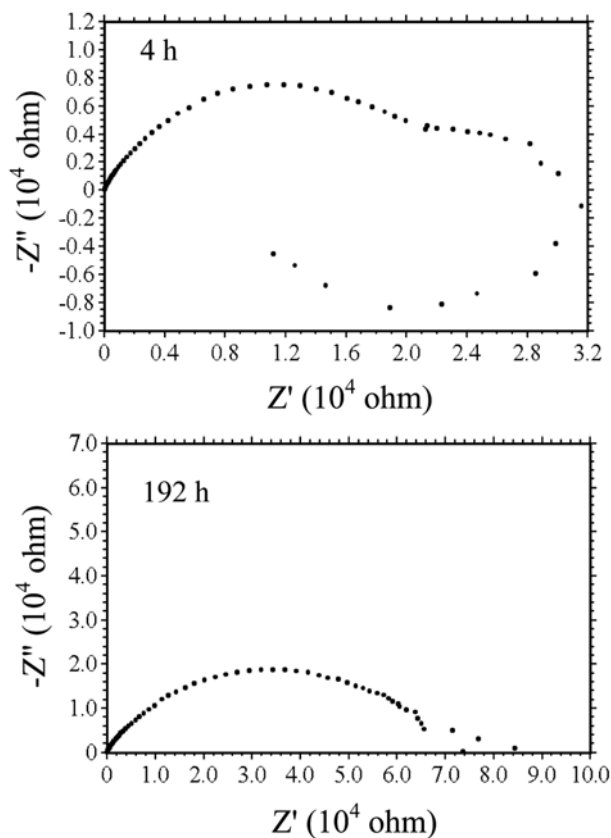


Fig. 9. The Nyquist diagrams recorded for CuZn electrode in 3.5% NaCl solution, after various exposure times.

semicircle observed at the high frequency region was determined as the charge transfer resistance (R_{ct}) that was responsible for the anodic dissolution of bare brass surface. The second one at medium frequency was related to the resistances of oxide layers (R_o) produced by copper. The inductive loop at low frequencies resulted from the adsorption of different corrosion intermediates which were due to the interplay between adsorption and electrodisolution [29]. This resistance resulted from nonhomogeneous structure which consisted of a different surface structure in view of micro-roughness and pore structure. It is well known that the polarization resistance consists primarily of capacitive components expanding from high to low frequency region and equals to total of resistance of capacitive components. A metal surface such as brass has copper and zinc surface structure. Consequently, the dissolution of brass electrode occurs on zinc metal rather than on the copper metal directly since the metallic copper is nobler than zinc metal against corrosion. This suggests that the resulting layer is richer in copper because of the oxidation of zinc contents in brass. Therefore, brass surface eventually has a configuration of copper oxides/substrates. According to previous proceedings [23-25,27], Nyquist plots recorded for bare copper did not exhibit an inductive loop as with bare brass electrode, in neutral conditions. Thus, it revealed that the dissolution of zinc led to formation of inductive resistance. In this study, the inductive loop disappeared after 192 h of immersion time. This Nyquist curve gave evidence of the presence of an effective barrier layer on the brass

surface. In this case, the barrier layer mainly consisted of copper and its oxides/substrates. This depressed semicircle consisting of charge transfer resistance (R_{ct}) against brass corrosion and oxide layer resistance was equal to polarization resistance (R_p) [23-25,27,30,31]. On the other hand, in presence of chloride ions, the formation of insoluble $CuCl$ layer rich in copper and complex $ZnO \cdot H_2O$ rich in zinc on brass surface contributed to an increase in polarization resistance. In addition, the oxidation of $Cu(I)$ to $Cu(II)$ caused the formation of soluble products such as $CuCl_2$ and $CuCl^+$ complex ions. Consequently, further growth of oxide, soluble and insoluble layer on the brass surface provided an increase in R_p value, after 192 h of exposure time.

Fig. 10 shows the Nyquist plots recorded for the POA-coated electrodes after various exposure times in 3.5% NaCl solution. 4 h after the immersion time, there were two depressed semicircles which could not be well resolved for $CuZn/POA-L$ and one depressed semicircle for $CuZn/POA-H$ in Nyquist plots. In the case of $CuZn/POA-L$ coating system, the Nyquist plot consisted of two depressed semicircles at high and low frequencies region. It was also clear that two plateau regions were observed in the $\log f$ - $\log Z$ diagram (Fig. 11(a)). The first semicircle was related to charge transfer resistance (R_{ct}) at metal/polymer interface within the pores of the polymer film. The second one included the polymer film (R_f) and the oxide layer resistance (R_o). The sum of these resistances was equal to polarization resistance (R_p) ($R_p = R_{ct} + R_f + R_o$) [23,25-27,30,31]. On the other hand, the depressed semicircle at high and low frequency regions was attributed to charge transfer resistance, oxide film and polymer film resistances, the sum of which was equal to polariza-

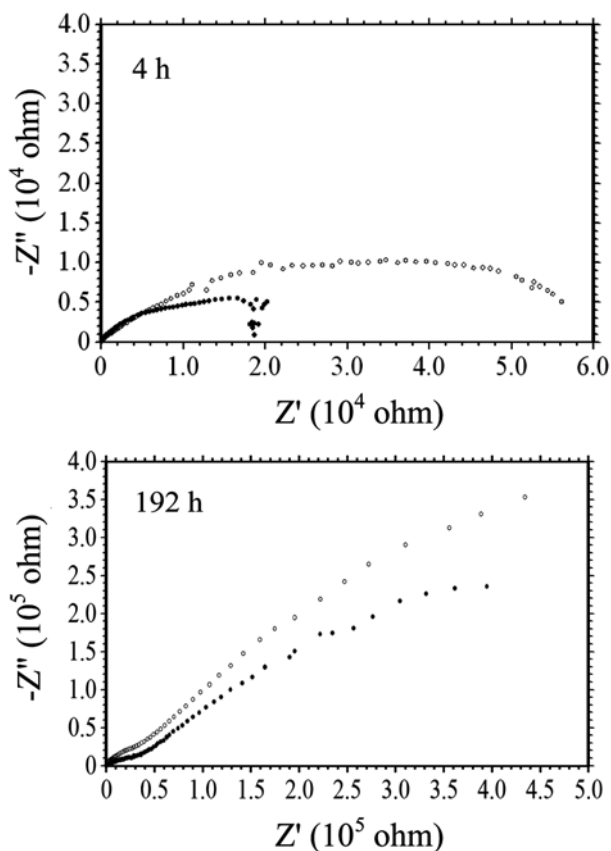


Fig. 10. The Nyquist diagrams recorded for $CuZn/POA-L$ (●) and $CuZn/POA-H$ (○) electrodes in 3.5% NaCl solution, after various exposure times.

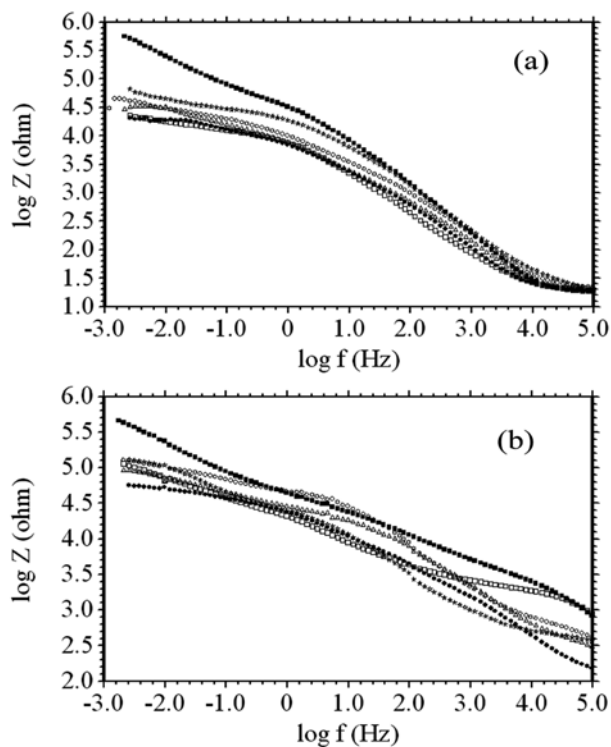


Fig. 11. The $\log Z$ vs. $\log f$ plots recorded for $CuZn/POA-L$ (a) and $CuZn/POA-H$ (b) after (●) 4 h, (△) 24 h, (○) 48 h, (×) 96 h, (■) 192 h and (□) 240 h of immersion time in 3.5% NaCl.

tion resistance (R_p) for CuZn/POA-H. These R_p values of the CuZn/POA-L and CuZn/POA-H electrodes were found to be approx. 18.6 and 52.6 kW 4 h after the exposure time, respectively. It is clearly seen from Fig. 10 that polymer-coated electrodes did not exhibit inductive behavior. It is clear that the polymer films synthesized at both scan rates on brass electrode provided an efficient barrier property against the corrosive products. The R_p values of these coated electrodes increased in 192 h of immersion time due to the increase in the amount of electrolyte solution within polymer coating (Fig. 10). This was explained by the oxidizing behavior of polymer film, which led the formation of some passive layers such as CuO and Cu₂O. Consequently, this catalytic property of polymer film contributed anodic protection to brass. It is well known that semi-circles which appear in Nyquist diagrams occur due to a condenser system building up at the metal/solution interface. In an actual condenser, both layers are controlled by electrons. However, where certain oxidizable metals such as iron, copper and brass do not act like a real condenser, the charge distribution is controlled by electrons on the metal side of the double layer but by ions on the solution side. Hence, metal under polymer coated electrode dipped in 3.5% NaCl solution dissolved under the effect of chloride ions diffused by the double layer resulting in electron accumulation while polymer film was reduced at metal/polymer interface. These two events contributed to the resistance feature of the metal. In relevant log f-log Z diagrams (Fig. 11(b)), the clarity of charge transfer resistance observed for CuZn/POA-H electrode could be explained by conversion of copper from anodic oxidation to its oxides under the catalytic effect of polymer film as discussed in here. Yet, the increase in R_{ct} value for CuZn/POA-L electrode was not clearly identified (Fig. 11(a)). The formation of protective passive layers was possible with limited ion diffusion. Therefore, the different synthesis condition led to the diverse porous structures of polymer films which exhibited different catalytic behaviors on the electrode surface. In this study, the low permeability of CuZn/POA-H electrode was observed from the higher R_p values indicating an increase in barrier properties of polymer film, in longer immersion time. On the other hand, the R_p value of CuZn/POA-L electrode was found to be lower than that of CuZn/POA-H, while there was an increase in R_p values of CuZn/POA-L during following exposure time under catalytic behavior of polymer film. As a result, the POA coatings synthesized in two different scan rates exhibited an important physical protection on the brass surface and maintained the barrier property, in longer periods.

CONCLUSION

The synthesis of poly(o-anisidine) (POA) films on brass was carried out from neutral solution such as sodium oxalate by making use of cyclic voltammetry technique. The polymer films synthesized in sodium oxalate were homogeneous, compact and strongly adherent on brass electrode, with the application of two different scan rates. The scan rate applied for synthesis was a significant factor on the porous structure of POA films. The corrosion performance of POA coated electrodes was investigated by time-open circuit potential, anodic polarization curves and AC impedance spectroscopy. Electrochemical measurement results showed that POA films provided a physical barrier property to brass electrode. Rather less

porous structure of CuZn/POA-H electrode played an important role on some anodic protection, accelerating the formation of stable oxide layers, and the catalytic behavior of polymer film synthesized with high scan rate contributed to the effective barrier property, in longer periods.

ACKNOWLEDGMENTS

The research project was funded by The Scientific and Technical Research Council of Turkey (TUBITAK), Project No: TBAG-HD/135 (106T198).

REFERENCES

1. S. J. Kim, M. Okido and K. M. Moon, *Korean J. Chem. Eng.*, **20**, 560 (2003).
2. S. J. Kim, J.-II Kim and M. Okido, *Korean J. Chem. Eng.*, **21**, 915 (2004).
3. H.-J. Lee, D.-W. Kang and Y. J. Lee, *Korean J. Chem. Eng.*, **21**, 895 (2004).
4. B. Assouli, Z. A. Ait Chikh, H. Idrissi and A. Srhiri, *Polymer*, **42**, 2449 (2001).
5. R. Ravichandran and N. Rajendran, *Appl. Surf. Sci.*, **241**, 449 (2005).
6. F. M. Al-Kharafi, B. G. Ateya and R. M. Abd Allah, *J. Appl. Electrochem.*, **34**, 47 (2004).
7. S. Mamas, T. Kiyak, M. Kabasakaloglu and A. Koc, *Mat. Chem. Phys.*, **93**, 41 (2005).
8. M. M. Antonijević, S. M. Milić, S. M. Šerbula and G. D. Bogdanović, *Electrochim. Acta*, **50**, 3693 (2005).
9. G. Kousik, S. Pitchumani and N. G. Renganathan, *Prog. Org. Coat.*, **43**, 286 (2001).
10. A. J. Motheo, M. F. Pantoja and E. C. Venancio, *Solid State Ionics*, **171**, 91 (2004).
11. S. K. Mondal, K. R. Prasad and N. Munichandraiah, *Synth Met.*, **148**, 275 (2005).
12. A. M. Fenelon and C. B. Breslin, *Surf. Coat. Tech.*, **190**, 264 (2005).
13. V. Rajendran, A. Gopalan, T. Vasudevan, W. C. Chen and T. C. Wen, *Mat. Chem. Phys.*, **65**, 320 (2000).
14. N. M. Martyak, P. McAndrew, J. E. McCaskie and Dijon, *Prog. Org. Coat.*, **45**, 23 (2002).
15. V. Shinde, S. R. Sainkar and P. P. Patil, *J. Appl. Polym. Sci.*, **96**, 685 (2005).
16. P. A. Kilmartin, L. Trier and G. A. Wright, *Synth Met.*, **131**, 99 (2002).
17. A. Eftekhari, *Synth Met.*, **145**, 211 (2004).
18. D. D. Borole, U. R. Kapadi, P. P. Mahulikar and D. G. Hundiwale, *Polym-Plast Technol. Eng.*, **43**, 1443 (2004).
19. P. Pawar, M. G. Wankhede, P. P. Patil and S. R. Sainkar, *Mat. Sci. Eng. A*, **347**, 365 (2003).
20. Pourbaix, *Atlas of electrochemical equilibria in aqueous solutions*, NACE, Houston, Texas (1966).
21. A. T. Ozyilmaz, N. Çolak, G. Ozyilmaz and M. K. Sangün, *Prog. Org. Coat.*, **60**, 24 (2007).
22. A. M. Fenelon and C. B. Breslin, *Synth. Met.*, **144**, 125 (2004).
23. A. T. Ozyilmaz, T. Tüken, M. Erbil and B. Yazıcı, *Prog. Org. Coat.*, **52**, 92 (2004).
24. A. T. Ozyilmaz, *Prog. Org. Coat.*, **54**, 127 (2005).
25. A. T. Ozyilmaz, N. Çolak, M. K. Sangün, M. Erbil and B. Yazıcı,

- Prog. Org. Coat.*, **54**, 353 (2005).
26. A. T. Ozyilmaz, G. Kardaş, M. Erbil and B. Yazıcı, *Appl. Surf. Sci.*, **242**, 97 (2005).
27. A. T. Ozyilmaz, *Surf. Coat. Tech.*, **200**, 3918 (2006).
28. S. Patil, S. R. Sainkar and P. P. Patil, *Appl. Surf. Sci.*, **225**, 204 (2004).
29. F. Mansfeld, *Corrosion*, **35**, 301 (1981).
30. F. Mansfeld, *J. Appl. Electrochem.*, **25**, 187 (1995).
31. G. W. Walter, *Corrosion*, **26**, 681 (1986).